Shared Control for the Nonlinear Dynamic Model of a Car-like Robot

Shirui Song*

Faculty of Engineering and Physical Sciences, University of Southampton, Southampton SO17 1BJ, United Kingdom

*ss9e21@soton.ac.uk

Abstract

In this paper we study the shared control problem for a car-like robot and derive a feedback controller which guarantees the safety of the robot in the presence of stationary obstacles. The actual shape of the robot is explicitly considered by defining an appropriate distance to be used in the control design. It is shown that the use of dynamic extension plus partial feedback linearization allows constructing a Lyapunov function from which a safe controller can be designed. Simulations results on the model of rear-wheel-driving and front-wheel-driving cars are used to validate the theoretical development.

Keywords

Car-like robot, nonlinear control, obstacle avoidance, dynamic feedback linearization.

1. Introduction

Car-like robots are a type of robots constructed to resemble, or function similarly, to a car, with a chassis, wheels, steering mechanism, and sensors [1]. These can be used in transportation services like self-driving taxis, delivery services, and can navigate complex environments to transport goods and passengers. To establish a simple model, we assume that the two wheels on the rear axle are aligned with the car, and the front wheels can turn while the rear wheel direction is fixed [2].

At present cars are mainly driven by operators, but in an autonomous environment or dangerous situations feedback controllers should take over to guarantee safety. Therefore, the design of a shared controller aimed at combining the reliable performance of feedback controllers with the adaptive capabilities of operators is of practical importance.

Many different feedback controllers have been proposed for car-like robot. In particular, [3] has proposed a novel multi-delay proportional integral retarded (PIR) control which is such that the tracking error asymptotically converges to zero and potential harmful high-frequency measurement noise is attenuated through the delay term. Reference [4] proposed a collaborative control scheme for the vehicle motion model of the rear-wheel drive where the Cartesian position set achievable is characterized by a sequence of linear inequalities. Paper [5] has come up with a practical tracking controller that uses second-order sliding mode technology through the super-twisting algorithm. Dynamical surface control methodology was used in [6] to reduce controller complexity and guarantee predetermined transient and steady-state performance with collision and singularity prevention by performance constraint methods. Moreover, [7] introduced a control plan for autonomous car-like robots that combines potential fields and neuro-evolutionary controllers along with the training environment.

Finally, [8] has introduced a new universal feedback control framework that deals with finite and unbounded domains among possible steering angle domains for car-like robots.

This work aims at establishing a feedback controller for both the front-wheel drive and rear-wheel-drive dynamic models of car-like robots. This is done by setting up a safe distance that will take into consideration the size of the vehicle during design and a human operator with a feedback controller to have a common control system, a method that was used in [2] and [4]. The use of dynamic extension advocated in the paper allows partially to extend the proposed design to systems composed by a car with trailers. Finally note that we do not limit obstacles to be such that the robot moves in a convex environment, but directly achieve obstacle avoidance by measuring the distance between the robot and the obstacles, making this design more flexible and applicable to practical scenarios.

The rest of the paper is organized in the following way. Section II provides the formulation of the control problem. In sections III and IV, the dynamic models of the rear-wheel-drive and front-wheel-drive devices are presented respectively. In these parts, the distance depending on the shape of the car is identified and the safety controller and the shared control algorithm are discussed in detail. Section V presents the results of the shared control, through the application of two case studies, which are used to illustrate how the shared control works. Lastly, Section VI contains the conclusions and recommendations for future work.

2. Problem Formulation

In this part, the common control issue is determined. We use *h-control* and *f-control* to indicate the human-initiated behavior and feedback control respectively and establish two variables uh and uf. Furthermore, the sharing flotation k $\in$ [0, 1] is presented to measure the distribution of the control to uh and uf .

To describe the overall set of feasible values for the state, we divide the state space into a *safe subset* and a *dangerous subset*. Informally, if the state belongs to an ”extended” (to be defined) safe subset, we set k = 1. If the state belongs to an ”extended” (to be defined) dangerous subset, we set k = 0. The car-like robot is made to receive the input for the variable k which is the shared control signal us , which is based on the transformation of the feedback control input uf and the human input uh.

In that context, the research problem can be formulated as follows: Using an admissible configuration set PA , and a predetermined *h-controller*, identify the following

$$\begin{cases} f-controller\ u_f, \\ Sharing\ function\ k, \\ Safe\ set\ \mathcal{R}_{\mathcal{S}}, \end{cases} \tag{1}$$

In this case, RS ≜ PA × AS × V1S × V2S ⊂ PA × A × V1 × V2 ≜R, with A is the set of all heading angles, and AS is the set of the heading angles where the robot is unable to access the boundary of PA in some arbitrarily short time period. V1 and V2 similarly represent driving speeds and steering speeds, respectively. The common control system is intended to have the following properties.

$$\begin{cases} \mathcal{R}\ is\ forward\ invariant, \\ \Omega_s = \begin{cases} \Omega_h & if\ \Omega_h \subset \mathcal{R}_{\mathcal{S}}, \\ \Pi_{\mathcal{R}_{\mathcal{S}}}(\Omega_h) & if\ \Omega_h \not\subset \mathcal{R}_{\mathcal{S}}, \end{cases} \\ u_s = u_h\ if\ the\ system\ is\ in\ \mathcal{R}_{\mathcal{S}}. \end{cases} \tag{2}$$

Note that heading angles and velocities are formally introduced in Section 3 and 4.

3. Safe Control for A Rear-Wheel-Driving Model of a Car-Like Robot

In this section we recall the kinematic model of a rear-wheel-driving car [1], describe the dynamic extension and the partial feedback linearization steps implemented, and define the distance function instrumental for the design of the shared controller.

3.1. Kinematic Model

We can take an example of a robot that applies the kinematic laws of a car, as shown in Figure 1. The two wheels on an axle (front and rear) are simplified as one wheel, which is placed at the center of the axle (using the model of a car). The front wheel can be steered, but the rear wheel does not. The generalized coordinates are further printed as q = (x, y, theta, phi). x and y reflect the Cartesian coordinates of the back wheel, the angle theta of the automotive body against the x-axis is theta, and the angle phi of the steering wheel is phi.

If the car has rear-wheel driving, the kinematic model is given by the equations [1].

$$\begin{cases} \dot{x} = \cos\theta\, v_1, \\ \dot{y} = \sin\theta\, v_1, \\ \dot{\theta} = (\tan\phi/l)\, v_1, \\ \dot{\phi} = v_2, \end{cases} \tag{3}$$

where *v1* and *v2* are the driving and the steering velocity input, respectively.

3.2. Dynamic Extension, Coordinate Transformation, and Feedback Linearization

To simplify the control design, we add one integrator to the input channel *v1* and define the new coordinate.

$$\dot{\theta} = \frac{\tan\phi}{l}\, v_1, \tag{4}$$

which is such that

$$\ddot{\theta} = \frac{1}{\cos^2\phi\, l}\, v_2 + \frac{\tan\phi}{l}\, \dot{v}_1, \tag{5}$$

Setting v1 = u1 and θ‟ = u2 , yields

$$\begin{cases} \dot{x} = \cos\theta_1\, v_1 \\ \dot{y} = \sin\theta_1\, v_1, \\ \dot{\theta}_1 = \theta_2, \\ \dot{v}_1 = u_1, \\ \dot{\theta}_2 = u_2, \end{cases} \tag{6}$$

which is the model used in the controller design. Note that this resembles the dynamic model in (6).

3.3. Definition of Distance Function

Since there is no possibility to acquire absolute position measurements, one is only able to determine the distances to obstacles and the angular difference between the reference heading

angle and the actual one. Consequently, the system dynamics need to be reformulated with the variables *d = [d1, d2]^T*. In this case, *d1* is the distance of the closest obstacle to the direction of the reference velocity, *d2* is the distance of the closest obstacle to the direction of the reference velocity.

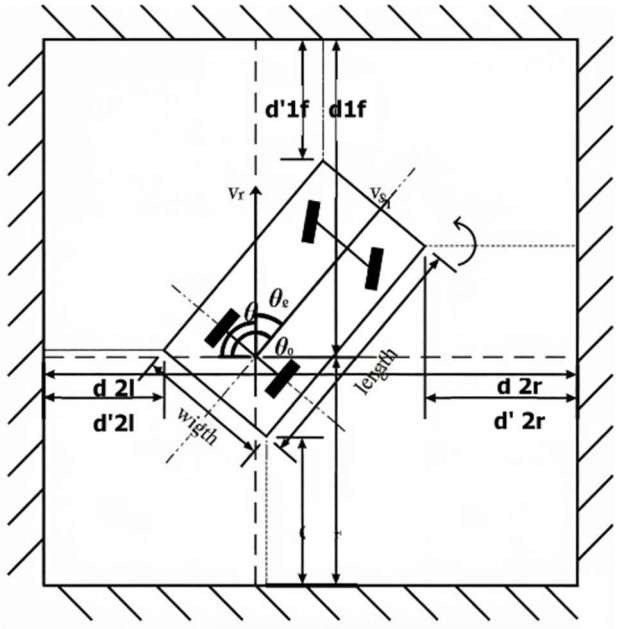

Fig. 1 The model of a rear-wheel-driving car. Shadowed region: not admissible set; vr: reference forward velocity; θr: reference heading angle

When controlling the car, its shape needs to be considered, as the size of the car can affect its maneuverability and handling, hence one has to ensure that the car-like robot has sufficient space and mobility during turning, parking, lane changing, saintuations. For our simulations, the car-like robot is considered to be a rectangle of dimension *length x width.*

Using simple geometrical consideration, as illustration in Fig. 2 and 3.

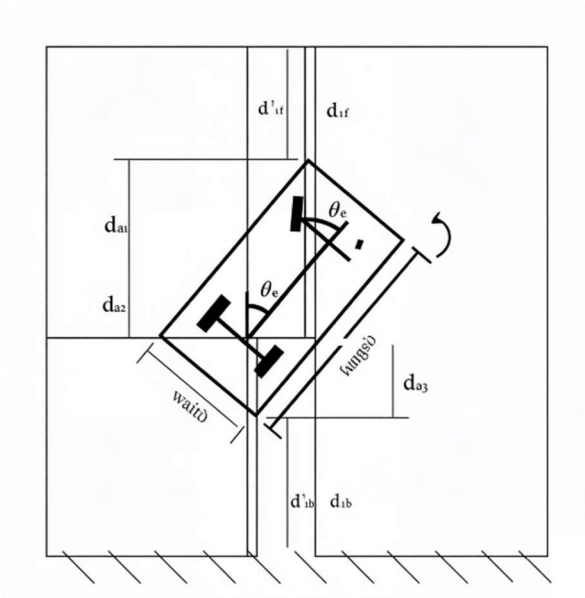

Fig. 2 Definition of the front and back distance variables for a rear- wheel-driving car

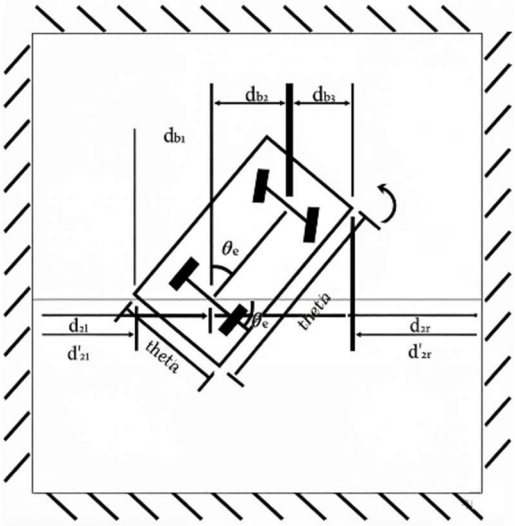

Fig. 3 Definition of the left and right distance variables for a rear- wheel-driving car.

Note that when $\theta_e = 0$ and $\theta_e = \pi/2$, some of the variables introduced are not defined. For clarity we illustrate these cases in Fig. 4 and 5, and summarize the results in Table 1.

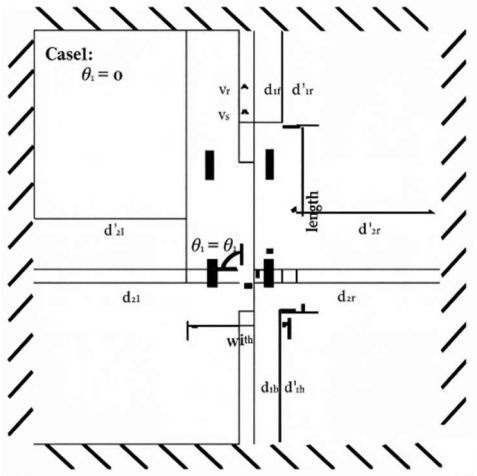

Fig. 4 Distance variable for θe = 0.

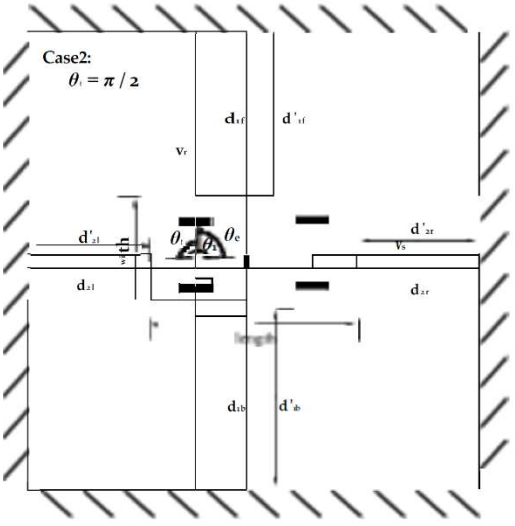

Fig. 5 Distance variable for θe = π/2

Table 1. summary of the distance variables for *θe= 0 and θe= π/2* for a rear-wheel-driving car

	0	π/2
Front	3/4 length	1/2 width
Back	1/4 length	1/2 width
Left	1/2 width	1/4 length
Right	1/2 width	3/4 length

The values of the δ variable are plotted in Fig. 6, for the case *length = 0.4*, and *width = 0.2*

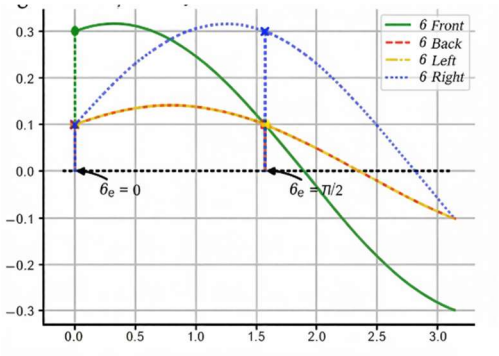

Fig. 6 The δ variables for a rear-wheel-driving car as a function of *θe*.

We complete this section by defining the vectors $d = [d1, d2]^T$, $da = [d_{1f}, d_{2l}]^T$, and $db = [d_{1b}, d_{2r}]^T$, where thevariables are defined in equations (3)-(6).

3.4. Design of the Feedback Controller

To design the feedback controller, similar to [4], we define new variables drj, j ∈ {1, 2}, which takes into account the shape of the robot and the environment.as

$$d_{rj} = \begin{cases} d_{dj}, & if\ d_{dj} \geq (1-\sqrt{2}/2)r + \epsilon. \\ \epsilon, & if\ d_{dj} \leq (1-\sqrt{2})r + \epsilon. \\ m_j, & otherwise. \end{cases} \tag{7}$$

In addition we define

$$\theta e = \theta\, 1 - \theta r\,, \tag{8}$$

$$z_j = \log \frac{d_i^{'}}{d_{rj}},\ d_i^{'} \in (d_{1f}^{'}, d_{2l}^{'}). \tag{9}$$

Using these variables yields the equations

$$\begin{cases} \dot{z}_1 = \dot{d}_{1f}^{'}/d_{1f}^{'} - \dot{d}_{r1}/d_{r1} = v_{1r}/d_{r1} - v_1 \cos\theta_{1e}/d_{1f}^{'}, \\ \dot{z}_2 = \dot{d}_{2l}^{'}/d_{2l}^{'} - \dot{d}_{r2}/d_{r2} = -v_1 \sin\theta_{1e}/d_{2l}^{'}, \\ \dot{\theta}_{1e} = \theta_{2e}, \\ \dot{v}_1 = u_{1f}, \\ \dot{\theta}_{2e} = u_{2f} - u_{2r}, \end{cases} \tag{10}$$

where ur = [u1r, u2r]T = [d“r1 , θ“r]T is the reference input signal. Let $\dot{\theta}_e(t)$ describe the desired value for θe at the time instant t, consider a point (dd ,θ 1d, v1d,θ2d) in the Ω-limit set of the *closed-loop system*, and define the projection of (dd ,θ 1d, v1d,θ2d) into RS as

$$\Pi RS\ (dd\ ,\theta\ 1d,\ v1d,\theta 2d) = (dr\ ,\theta\ 1r,\ v1r,\theta 2r). \tag{11}$$

Let

$$\theta_{1e}^{*} = atg(\gamma_2 d_{2l}^{'} z_2, d_{1f}^{'}(\frac{v_{1r}}{d_{r1}} + \gamma_1 z_1)), \tag{12}$$

$$v_1^{*} = \sqrt{(d_{1f}^{'}(\frac{v_{1r}}{d_{r1}}) + \gamma_1 z_1)^2 + (\gamma_2 d_{2l}^{'} z_2)^2} \tag{13}$$

$$\theta_{2e}^{*} = \dot{\theta}_{1e}^{*} - \frac{z_1 v_1^{*}}{d_{1f}^{'}} \sin\frac{\theta_{1e} + \theta_{1e}^{*}}{2} sinc\frac{\theta_{1e}^{i} - \theta_{1e}^{*}}{2} + \frac{z_2^{i} v_1^{*}}{d_{2l}^{'}} \cos\frac{\theta_{1e} + \theta_{1e}^{*}}{2} sinc\frac{\theta_{1e} - \theta_{1e}^{*}}{2}. \tag{14}$$

Then consider the Lyapunov function candidate

$$L(z_1, z_2, \theta_{1e}, v_1, \theta_{2e}) = \frac{1}{2}[z_1^2 + z_2^2 + (\theta_{1e} - \theta_{1e}^{*})^2 + (v1 - \dot{v}1)2 + (\theta 2e - \dot{\theta}2e)2]. \tag{15}$$

Evaluate the time derivative of L along the trajectories of the system (10) and setting

$$u_{1f} = \dot{v}_1^{*} + \frac{z_1}{d_{1f}^{'}} \cos\theta_{1e}^{i} + \frac{z_2}{d_{2l}^{'}} \sin\theta_{1e} - \gamma_3(v_1 - v_1^{*}) \tag{16}$$

$$u2f = u2r + \dot{\theta}.2e - \dot{\theta}\ 1e + \dot{\theta}\ 1e - \gamma 4\ (\theta 2e - \dot{\theta}2e). \tag{17}$$

yields

$$L. = -\gamma 1\ \dot{z}1^{2} - \gamma 2\ \dot{z}2^{2} - \gamma 3\ (v1 - \dot{v}1)2 - \gamma 4\ (\theta 2e - \dot{\theta}2e)2 \leq 0, \tag{18}$$

which is negative semi-definite. Note that the feedback control (16)-(17) can be written as

$$u_{1f} = \dot{v}_1^{*} + \frac{\log\frac{d_{1f}^{'}}{d_{r1}}}{d_{1f}^{'}} \cos\theta_{1e}^{i} + \frac{\log\frac{d_{2l}^{'}}{d_{r2}}}{d_{2l}^{'}} \sin\theta_{1e} - \gamma 3\ (v1 - \dot{v}1) \tag{19}$$

$$u2f = u2r + \dot{\theta}.2e - \dot{\theta}\ 1e + \dot{\theta}\ 1e - \gamma 4\ (\theta 2e - \dot{\theta}2e). \tag{20}$$

3.5. Design of the Shared Control Law

For any given human input vh , the *safe subset* and the *dangerous subset* [4], RS and RD, are redefined as

$$RS(vh) = \{(d_{1f}, d_{2l}, \theta e + \theta r) \in R+ \times R+ \times S, \quad (21)$$

where $vh \leq 1/(b2 - D) - 1/(b2)$, if $D \leq b2$.

$$RD(vh) = \{(d_{1f}, d_{2l}, \theta e + \theta r) \in R+ \times R+ \times S, \quad (22)$$

where $vh \geq 1/(b1 - D) - 1/b1$ and $0 \leq D \leq b1\}$. D is the distance to the obstacle along the direction of vh, and $b2 > b1 > 0$ are user selected parameters. The shared controller relies on the definition of the variable

$$k(D, v_h) = \begin{cases} 1, & (d'_{1f}, d'_{2l}, \theta_e) \in \mathcal{R}_S(v_h), \\ 0, & (d'_{1f}, d'_{2l}, \theta_e) \in \mathcal{R}_D(v_h), \end{cases} \quad (23)$$

which gives the control signal

$$us = (1 - k(D, vh))uf(da, dr, \theta 1e, v1, \theta 2e\theta 1r, v1r, \theta 2r, ur) + k(D, vh)uh. \quad (24)$$

Proposition1: Consider the rear-wheel-driving model of the car-like robot with the feedback controller given by (19)-(20) and (24). Let $P(0) = [x(0), y(0)]^T \in PA$ and let uh be the human controller. The shared-controlled system has the following properties.

(1) us (t) = uh (t) when the state of the system is in RS .

(2) uf is bounded.

(3) P(t) stays in PA for all $t \geq 0$.

(4) $\Omega s = \Pi RS(\Omega h)$.

Proof : Property (1) states that the human controller is active in RS .

Note that the uf is bounded, since it is a continuous function of bounded variables, hence property (2) holds.

To check property (3), see that L is positive definite, and that dL along the trajectories of the system is negative semidefinite. Additionally, based on the definition of RD, any trajectory will land in the perilous part of RD and leave R, in uf feedback control is turned on, which makes the set R forward-invariant. Thus, property (3) is satisfied.

When $\Omega h \subset RS$, by the assumption of human controller and the definition of feedback controller in equation (7)-(9) and (15), Ωh is the Ω-limit set of both the human controller and feedback controller. And in fact, in this case, this property is obtained from the general result in [9]. In case $\Omega h \not\subset RS$, Ω- limit set of the feedback controller is $\Pi RS(\Omega h)$, Using the definitions (21) and (22), the trajectory of the system reaches RD, where the uf is working. This pushes the system states into RS and is allowed to exit the admissible set R. Therefore, property (4) holds.

4. Safe Control for A Front-Wheel-Driving Model of A Car-Like Robot

In this section, a safety controller and a shared control law for the front-wheel-driving car-like robot are designed, which have all the properties presented in Section III.

4.1. A. Kinematic Model

Similar to Section III-A, when the car has front-wheel driving, the kinematic model is given by (25), where the driving velocity v1 refers now to the front wheel.

$$\begin{cases} \dot{x} = \cos\theta \cos\phi \, v_1, \\ \dot{y} = \sin\theta \cos\phi \, v_1, \\ \dot{\theta} = (\sin\phi / l) \, v_1, \\ \dot{\phi} = v_2. \end{cases} \tag{25}$$

4.2. Dynamic Extension, Coordinate Transformation, and Feedback Linearization

Consistently, we define the new coordinate with the addition of v1.

$$\dot{\theta} = \frac{\sin\phi}{l} \, v_1, \tag{26}$$

which is such that

$$\ddot{\theta} = \frac{\cos\phi}{l} \, v_2 + \frac{\sin\phi}{l} \, \dot{v_1}. \tag{27}$$

Then the dynamic extension was applied and change it into the following state variables. But it should be noted that in order to obtain a similar controller form, we use polar coordinate to do the transformation. To simplify the model, we set a = cosϕ v1 , where v1 ≠ 0, so the model of front- wheel-driving car can be describe in states (x, y,θ, θ. , a).
Setting a. = u1 and θ“ = u2 , yields

$$\begin{cases} \dot{x} = a \cos\theta_1 \\ \dot{y} = a \sin\theta_1, \\ \dot{\theta_1} = \theta_2, \\ \dot{a} = u_1, \\ \dot{\theta_2} = u_2, \end{cases} \tag{28}$$

which is the model used in the controller design. Note that this resembles the dynamic model in (28).

4.3. Definition of Distance Function

For the front-wheel-driving car (see Fig. 7), we define variable d = [d1 , d2]^T, and the δ variables for the same reason, which can be clearly seen from the geometric relationships in Fig. 8-9.

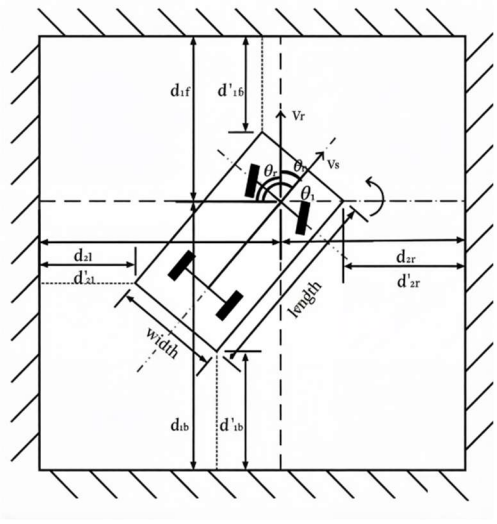

Fig. 7 The model of a front-wheel-driving car. Shadowed region: not admissible set; vr: reference forward velocity; θr: reference heading angle.

$$Front \begin{cases} d_{c3} = \sqrt{(1/4length)^2 + (1/2width)^2} \\ \cos\{\pi/2 - \theta_e - \arctan[(1/4length)/(1/2width)]\}, \\ \delta Front = d_{c3}, \\ d'_{1f} = d_{1f} - \delta Front. \end{cases} \tag{29}$$

$$Back \begin{cases} d_{c1} = (1/2width)/\sin\theta_e, \\ d_{c2} = \cos\theta_e[3/4length - (1/2width)/\tan\theta_e], \\ \delta Back = d_{c1} + d_{c2}, \\ d'_{1b} = d_{1b} - \delta Back. \end{cases} \tag{30}$$

$$Left \begin{cases} d_{d2} = \sin\theta_e[3/4length - (1/2width)\tan\theta_e], \\ d_{d1} = (1/2width)/\cos\theta_e, \\ \delta Left = d_{d1} + d_{d2}, \\ d'_{2l} = d_{2l} - \delta Left. \end{cases} \tag{31}$$

$$Right \begin{cases} d_{d3} = \sqrt{(1/4length)^2 + (1/2width)^2} \\ \cos\{\theta_e - \arctan[(1/4length)/(1/2width)]\}, \\ \delta Right = d_{d3}, \\ d'_{2r} = d_{2r} - \delta Right. \end{cases} \tag{32}$$

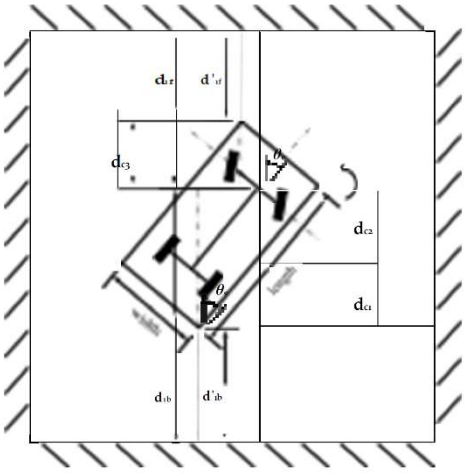

Fig. 8 Definition of the front and back distance variables for a front- wheel-driving car

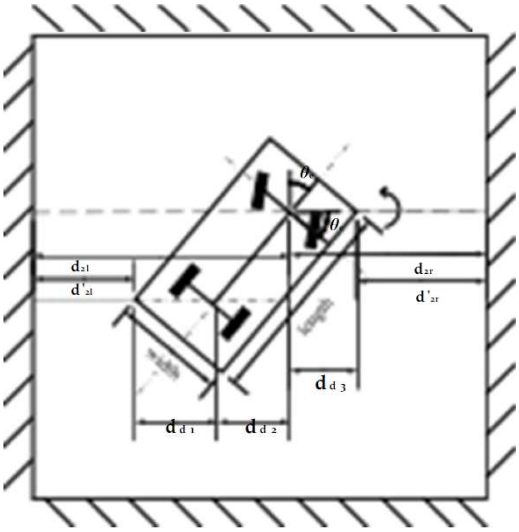

Fig. 9 Definition of the left and right distance variables for a front- wheel-driving car

Similar to the rear-wheel-driving car, we notes the values corresponding to these discrete points of θe = 0 and θe = π/2, then we summarize the results in Table 2.

Table 2. summary of the distance variables for θe = 0 and θe = π/2 for A front-wheel-driving car.

	0	π/2
Front	1/4 length	1/2 width
Back	3/4 length	1/2 width
Left	1/2 width	3/4 length
Right	1/2 width	1/4 length

and the behavior of δ for the front-wheel-driving car is summarized in Fig. 10 for the case length = 0.4, and width = 0.2.

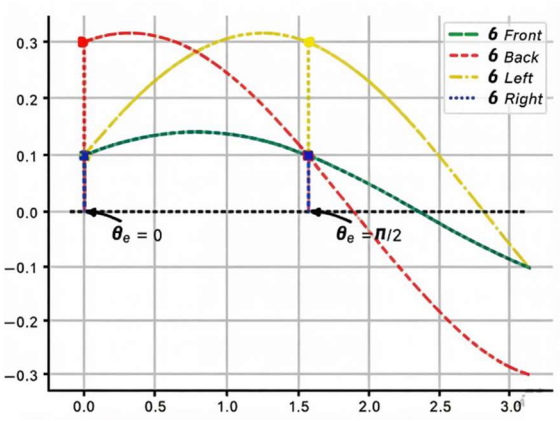

Fig. 10 The δ variables for a front-wheel-driving car as a function of θe

For the same reason, we complete this section by defining

the vectors d = [d1 , d2]^T , da = [d_{1f} , d_{2l}]^T , and db =[d_{1b} , d_{2r}]^T , where the variables are defined in equations (29)- (32).

4.4. Design of the Feedback Controller

The variables dr and z have defined in (7) and (9), re- spectively. Then the model of front-wheel-driving car with the variable z and θe can be described as.

$$\begin{cases} \dot{z}_1 = \ddot{d}'_{1f}/d'_{1f} - \dot{d}_{r1}/d_{r1} = a_r/d_{r1} - a\cos\theta_{1e}/d'_{1f}, \\ \dot{z}_2 = \ddot{d}'_{2l}/d'_{1f} - \dot{d}_{r2}/d_{r2} = -a\sin\theta_{1e}/d'_{1f}, \\ \dot{\theta}_{1e} = \theta_{2e}, \\ \dot{a} = u_{1f}, \\ \dot{\theta}_{2e} = u_{2f} - u_{2r}, \end{cases} \tag{33}$$

where ur = [u1r, u2r]^T = [d“r1 , θ“r]^T . Based on the variables previously derived, it can be mapped to the (d_{1f} , d_{2l} ,θ1 , a,θ2) coordinate as follow. Suppose (dd ,θ1d, ad ,θ2d) is a point of the Ω-limit set of the *h-closed-loop system*, and define the projection of (dd ,θ 1d, ad ,θ2d) into RS as

$$\Pi RS\ (dd\ ,\theta\ 1d,\ ad\ ,\theta 2d) = (dr\ ,\theta\ 1r,\ ar\ ,\theta 2r). \tag{34}$$

Let

$$\theta_{1e}^{*} = atg(\gamma_2 d_{2l}^{'} z_2, d_{1f}^{'}(\frac{a_r}{d_{r1}} + \gamma_1 z_1)), \tag{35}$$

$$a^{*} = \sqrt{(d_{1f}^{'}(\frac{a_r}{d_{r1}}) + \gamma_1 z_1)^2 + (\gamma_2 d_{2l}^{'} z_2)^2}, \tag{36}$$

$$\theta_{2e}^{*} = \dot{\theta}_{1e}^{*} - \frac{z_1 a^{*}}{d_{1f}^{'}} \sin\frac{\theta_{1e} + \theta_{1e}^{*}}{2} sinc\frac{\theta_{1e}^{i} - \theta_{1e}^{*}}{2} + \frac{z_2^{i} a^{*}}{d_{2l}^{'}} \cos\frac{\theta_{1e} + \theta_{1e}^{*}}{2} sinc\frac{\theta_{1e} - \theta_{1e}^{*}}{2}. \tag{37}$$

Then consider the Lyapunov function candidate

$$\begin{aligned} L(z_1, z_2, \theta_{1e}, a, \theta_{2e}) = \frac{1}{2}[z_1^2 + z_2^2 + (\theta_{1e} - \theta_{1e}^{*})^2 \\ +(a - a^{*})^2 + (\theta_{2e} - \theta_{2e}^{*})^2]. \end{aligned} \tag{38}$$

Evaluate the time derivative of L along the trajectories of the system (31) and setting

$$u_{1f} = \dot{a}^{*} + \frac{z_1}{d_{1f}^{'}} \cos\theta_{1e}^{i} + \frac{z_2}{d_{2l}^{'}} \sin\theta_{1e} - \gamma_3(a - a^{*}), \tag{39}$$

$$u2f = u2r + \dot{\theta}_{2e}^{*} - \theta_{1e}^{*} + \dot{\theta}_{1e}^{*} - \gamma 4\,(\theta 2e - \theta 2e^{*}). \tag{40}$$

yields

$$\dot{L} = -\gamma 1\, \dot{z}1^{2} - \gamma 2\, \dot{z}2^{2} - \gamma 3\,(a - a^{*})^{2} - \gamma 4\,(\theta 2e - \dot{\theta}2e^{*})^{2} \leq 0, \tag{41}$$

which is also negative semi-definite. Note that the feedback controller (37)-(38) can be written as

$$u_{1f} = \dot{a}^{*} + \frac{\log\frac{d_{1f}^{'}}{d_{r1}}}{d_{1f}^{'}} \cos\theta_{1e}^{i} + \frac{\log\frac{d_{2l}^{'}}{d_{r2}}}{d_{2l}^{'}} \sin\theta_{1e} - \gamma_3(a - a^{*}), \tag{42}$$

$$u2f = u2r + \dot{\theta}_{2e}^{*} - \theta_{1e}^{*} + \dot{\theta}_{1e}^{*} - \gamma 4\,(\theta 2e - \dot{\theta}2e^{*}). \tag{43}$$

4.5. Design of the Shared Control Law

The definitions of RS and R are similar to that given in (40)-(41) except for that these two subsets are sets in (d_{1f} , d_{2l} ,θ 1de + θ1dr, ad ,θ2de + θ2dr). Therefore, the control.
signal is similarly given by

$$us = (1 - k(D, vh))uf\,(da, dr, \theta 1e, a, \theta 2e\theta 1r, v1r, \theta 2r, ur) + k(D, vh)uh. \tag{44}$$

Proposition2: Consider the front-wheel-driving model of the car-like robot with the feedback controller given by (42)- (43) and shared control law given by (44). Let P(0) =

$[x(0), y(0)]^T \in$ PA and let uh be the human controller. The shared-controlled system has the following properties.

(1) us (t) = uh (t) when the state of the system is in RS.

(2) uf is bounded.

(3) P(t) stays in PA for all t ≥ 0.

(4) Ωs = ΠRS (Ωh)

The proof process is almost the same as the shared control law of rear-wheel-driving car, so it is omitted here

5. Simulation Results

In this section, we discuss two case studies in a numerical simulation environment: one in a free driving scenario and one in which the robot is performing a point-to-point maneuver. In the first scenario, the driver of the car-like controller is required to aid free driving in a rectangular space preventing collision. In the second scenario, the controller is required to aid the human to drive from an initial position to a final position along a U-shaped corridor. The simulation results demonstrate the effectiveness of the design.

5.1. Free Driving

Consider the admissible PA = {(x, y)|1.5 ≤ x ≤ 5.5, −0.5 ≤ y ≤ 6}, and the dynamic models of rear-wheel- driving and front-wheel-driving car-like robots, as given by equations (2) and (26), respectively. In this case, the human drive in a free manner, and the resulting (x, y) trajectory is displayed by the red/dashed curve in Figure 11-12. Note that without controller the (x, y) trajectory exits the admissible set. The trajectory resulting from the use of the shared controller is represented by a blue/solid curve (rear-wheel-driving car), and by the yellow/dashed-and-dotted curve (front-wheel-driving car).

Note that when the car is within PA, it is completely controlled by the human. However when a part of the car (usually one of the corners) is about to come into contact with the boundary of PA, that is the red rectangle, the feedback controller takes over the car and keeps the path within PA. When the car travels away from the boundary of PA, its state enters the safe subset RS, the human controller takes over again. The time histories of all states and of the sharing function k are shown in Figures 13-15, which demonstrate the effectiveness of the shared control algorithm

5.2. Point-to-Point Maneuver

In this case, we assume the admissible configuration set PA of the U-shaped corridor as following, and the dynamic

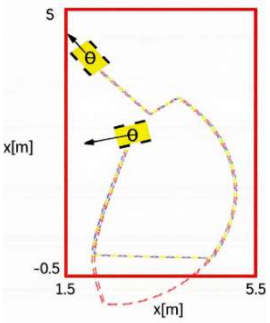

Fig. 11 (x, y) trajectories of the car: human control (red/dashed curve) shared control for the rear- wheel-driving car (blue/solid curve), and shared control for the front- wheel-driving car (yellow/dashed- and-dotted curve), in a free driving scenario.

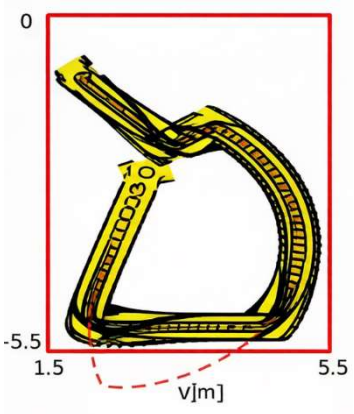

Fig. 12 Image of the rear/front- wheel-driving cars along their (x, y) trajectories in a free driving sce- nario.

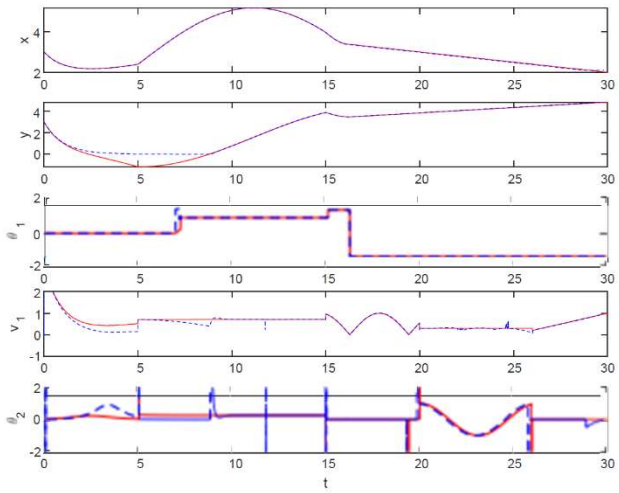

Fig. 13 Time histories of the state variables for the human control (red/solid line) and for the shared control (blue/dashed line) for the rear-wheel-driving car, in a free driving scenario.

models of rear-wheel-driving and front-wheel-driving car-like robots also given by equations(45), respectively.

$$\mathcal{P}_a = \left\{ (x,y) \;\middle|\; \begin{array}{l} 2 \le x \le 12, 0.5 \le y \le 10 \\ y \in [0.5, 3.9] \cup [6.9, 10] \text{ if } x \in [4.32, 9.57] \\ x \in [2, 4.32] \cup [9.57, 12] \text{ if } y \in [3.9, 6.9] \end{array} \right\} \tag{45}$$

The human need to perform a task from the initial position to the final position, and the resulting (x, y) trajectory is displayed by the red/dashed curve in Fig. 16-17. Note that without controller the (x, y) trajectory exits the admissible set. The trajectory resulting from the use of the shared controller is represented by a blue/solid curve (rear-wheel-driving car), and by the yellow/dashed-and-dotted curve (front-wheel-driving car).

Note that when the (x, y) trajectory of the human control passes through the not admissible region, while the trajectory

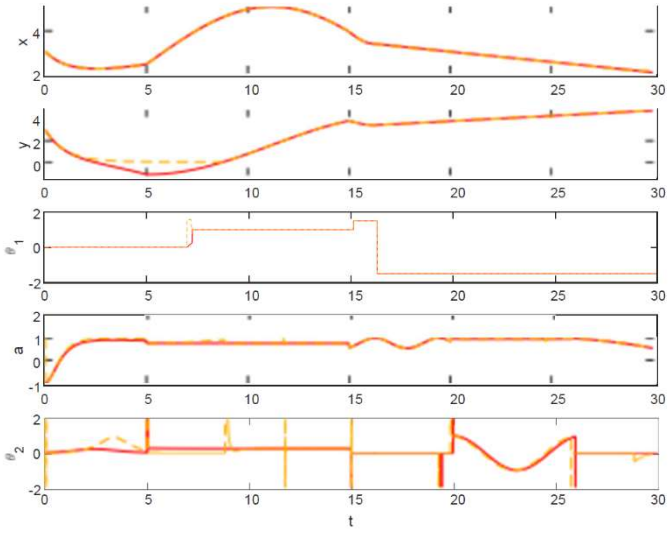

Fig. 14 Time histories of the state variables for the human control (red/solid line) and for the shared control (yellow/dashed line) for the front-wheel- driving car, in a free driving scenario

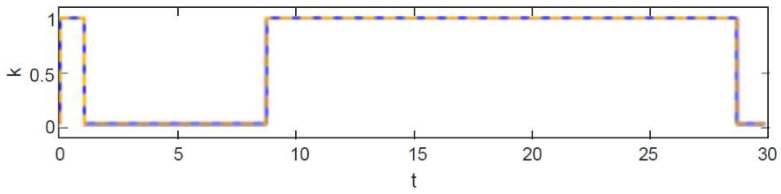

Fig. 15 Time history of the sharing function k for the rear-wheel-driving car (blue/solid line) and for the front-wheel-driving car (yellow/dashed line), in a free driving scenario

Fig. 16. (x, y) trajectories of the car: human control (red/dashed curve) shared control for the rear-wheel-driving car (blue/solid curve), and shared control for the front-wheel-driving car (yellow/dashed-and-dotted curve). Cyan square mark: the initial position of the robot. Green square mark: the final position of the robot with shared control, in a point-to-point maneuver scenario.

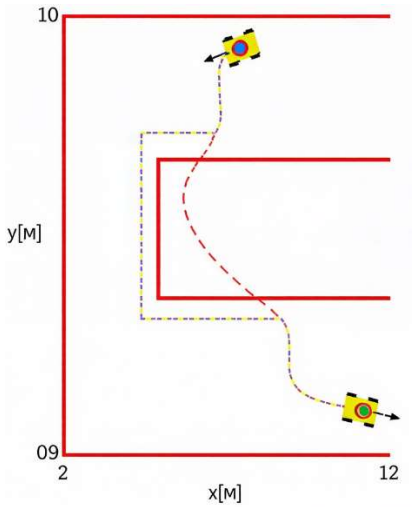

Fig. 16 Image of the rear/front- wheel-driving cars along their (x, y) trajectories for point-to-point mis- sion in a point-to-point maneuver scenario.

The shared control should moves along the boundary of PA until the human trajectory becomes feasible, the trajectory of the shared controller coincides with it again. The time histories of all states and of the sharing function k are shown in Figs 17-19.

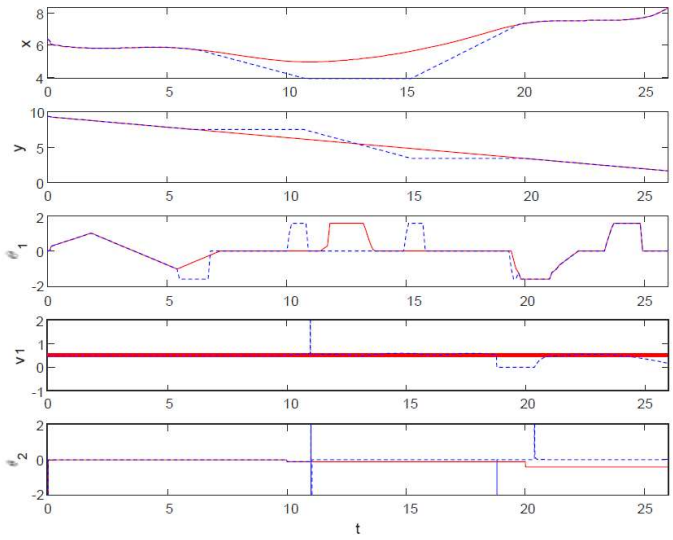

Fig. 17 Time histories of the state variables for the human control (red/solid line) and for the shared control (blue/dashed line) for the rear-wheel-driving car, in a point-to-point maneuver scenario

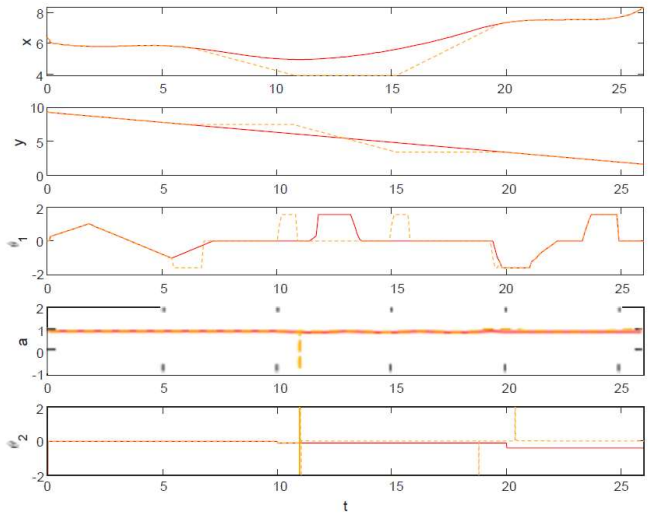

Fig. 18 Time histories of the state variables for the human control (red/solid line) and for the shared control (yellow/dashed line) for the front-wheel- driving car, in a point-to-point maneuver scenario.

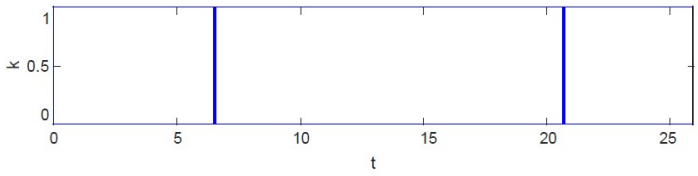

Fig. 19 Time history of the sharing function k for the rear-wheel-driving car (blue/solid line) and for the front-wheel-driving car (yellow/dashed line), in a point-to-point maneuver scenario.

6. Conclusion

This paper derives a safe feedback controllers for the dynamic models of rear-wheel-driving and front-wheel-driving car-like robots in an unknown environment. The actual shape of the robot has been considered to define a distance function which is then used in control design. A sharing function has been used to allocate the control authority to the human (when in safe conditions) or to the feedback controller (when in dangerous conditions). Simulation results in two scenarios have demonstrated the effectiveness of the designed safe feedback controller and shared controller. Future research will focus on the design of safety feedback controllers for car-like robots with n-trailers.

References

[1] A. De Luca, G. Oriolo, and C. Samson, "Feedback control of a nonholonomic car-like robot," Lecture Notes in Control and Information Sciences book series (LNCIS,volume 229), 2005.

[2] A. Astolfi, "Exponential stabilization of a car-like vehicle," Proceedings - IEEE International Conference on Robotics and Automation, Volume 2, Pages 1391-1396, 1995.

[3] J. Xu, C. Cai, Y. Niu, and H. Lam, "Genetic-Algorithm-Assisted Self-Scheduled Multidelay PIR Control: Experiments in a Car-Like Vehicle System," IEEE Transactions on Cybernetics, Volume 54, Issue 1, Pages 450-462, 2024.

[4] A. Cristofaro and T. A. Johansen, "Combining Obstacle Avoidance and Path Following in a Collision Avoidance Shared Control System," IFAC-PapersOnLine, Volume 54, Issue 20, Pages 196-201, 2021.

[5] M. M. M. Alves, L. C. A. Pimenta, and L. A. Torres, "A super-twisting sliding mode control strategy for car-like robots," 2021 IEEE International Conference on Robotics and Automation (ICRA), Pages 10266-10272, 2021.

[6] Y. Liu, J. Zhao, and G. Zhang, "Dynamical Surface Control for Car-Like Vehicles with Guaranteed Performance," IEEE Transactions on Vehicular Technology, Volume 70, Issue 6, Pages 5672-5683, 2021.

[7] A. E. B. Elhassani and S. A. A. Shah, "Autonomous Car-Like Robot Navigation Using Potential Fields and Neuro-Evolutionary Controllers," 2020 IEEE International Conference on Robotics and Automation (ICRA), Pages 8457-8463, 2020.

[8] A. Cristofaro, "A new universal feedback control scheme for car-like robots," Automatica, Volume 129, 109621, 2021.

[9] A. Cristofaro, T. A. Johansen, and A. R. Teel, "Combining Obstacle Avoidance and Path Following using the Shared Control Framework," 2020 IEEE Conference on Control Technology and Applications (CCTA), Pages 1128-1133, 2020.